

EIGHTEENTH EUROPEAN ROTORCRAFT FORUM

I - 01

Paper N° 54

**EXPERIMENTAL EVALUATION OF THE EH101 TAIL
ROTOR DYNAMICS IN FLIGHT**

**L. Luti, S. Scorbati, G. Vignati
AGUSTA S.p.A., ITALY**

**September 15-18, 1992
AVIGNON, FRANCE**

ASSOCIATION AERONAUTIQUE ET ASTRONAUTIQUE DE FRANCE

Curriculum Vitae

Luigi Luti got the degree in Aeronautical Engineering at the University of Rome, with a thesis on an experimental analysis of a rotor unsteady aerodynamic field. Then he collaborated to the Experimental and Applied Aerodynamics Department of University of Rome.

Two years ago he joined AGUSTA S.p.A., where he works in the Acustics and Vibration Department.

EXPERIMENTAL EVALUATION OF THE EH101 TAIL ROTOR DYNAMICS IN FLIGHT

L. Luti, S. Scorbati, G. Vignati
AGUSTA S.p.A.

Abstract

At the beginning of the EH101 Tail Rotor flight trials, the results obtained from the testing of EH101 helicopter Ground Testing Vehicle (GTV) and Prototypes indicate that the Tail Rotor lag frequencies drop rapidly as blade pitch is increased. It is of interest to examine the effects that some variables, as the imposed cuff pitch angle, exert on the mode frequencies.

Furthermore to help a better understanding of the rotor lag dynamics it is necessary to identify the specific rotor modes.

This paper reports two new procedures developed in AGUSTA, that have permitted the evaluation of the dynamic behaviour of the EH101 Tail Rotor.

1. Introduction

The main problem in the Tail Rotor design concerns the dynamic behaviour, and the environmental condition, in which it operates, significantly aggravates the situation.

The accurate determination of the dynamics of a Tail Rotor is an important task in order to ascertain lag load levels and stability margins. In fact, to minimize the lag loads, the natural frequency of the scissor mode and of the cyclic inplane mode should be well removed, respectively, from the $2 \times T_{Rev}$ and $1 \times T_{Rev}$ forcing. Moreover the cyclic lag frequency should intersect the $2 \times T_{Rev}$ inplane forcing at as small as possible pitch angle, in order to further reduce the involved energy.

The same problems were experienced during the early development phase of the EH101 helicopter Tail Rotor. The first configuration was a four bladed semirigid (flexible out-of-plane and rigid inplane) construction. Particularly its first

lag frequency (cyclic and scissor modes are coincident for this kind of rotor) intersects the $2 \times T_{Rev}$ inplane forcing at high cuff pitch angle value, with the result of high lag loads and hence high stresses.

Then a teetering Tail Rotor configuration was tested (see Fig. 1).

A dedicated experimental analysis was requested on the Ground Testing Vehicle and on Prototype, to confirm the theoretical prediction.

An attempt at identifying the natural lag frequencies had been made, by real time analysis in telemetry, using a portable single channel spectrum analyzer. The identification of the lag frequencies was made trying to recognize the differences in amplitude occurring when a pedal input was applied during a steady condition. Unfortunately this approach was highly influenced by the operator experience and his personal background.

A new analysis method, based both on different instrumentation for acquisition and data storage, was so defined to reduce this uncertainties and to allow a more effective data manipulations. A 3D and a contour plot formats were introduced for a data global visualization and verification. This method was called the Frequencies Identification Method (FIM).

However the abundance of forcing and fuselage frequencies in the range of interest between 1 and $3 \times T_{Rev}$ can lead to different interpretations of the dynamic behaviour of the rotor. To definitely solve out this problem the Frequencies and Operational Shapes Identification Method (OSIM) was introduced. This method, by means of a running mode analysis, allows a complete correct evaluation of the natural frequencies and the full identification of the related shapes. A dedicated set of instrumentation on the four arms of the hub was identified and installed. The limited number of the available

parameters of the GTV run allowed only the FIM, but the complete set of instrumentation installed on the prototype permitted both the FIM and OSIM.

2. Acquired Parameters

The following parameters were acquired:

- Beam bending and chord bending for every blade (only one for GTV);
- Hub bending (no for GTV);
- Pitch control rod bending for every blade (no for GTV).

All parameters were recorded in telemetry with a good phase relationship ($\leq 5^\circ$) in the interesting frequency range. Furthermore, for the prototype testing, all parameters were normalized with respect to their 50 hours stress limit values.

3. Flight Conditions

In order to clearly see the effects of the imposed pitch angle on the Tail Rotor lag dynamic, all the above mentioned parameters were acquired for a certain number of operational conditions, which gave a complete range of pitch angle values:

For tests performed on GTV:

- Stabilized condition at pitch angle from zero to full left pedal (26°).
- Pedal impulses (2° of pitch reduction, i.e. $10^\circ-8^\circ-10^\circ$).

For flight trials of Prototype:

- Hover OGE;
- Forward flight at different speeds up 150 kts;
- Right and left side flights.
- Right and left rotations (-3, -4, +2, +4, +6).

4. Procedure Description

The two methods are described in the following.

The starting point is the same for both the analyses: the parameters recorded in telemetry.

Frequency Identification Method - The beam and chord bending of only one blade are used. By the use of a analyzer these parameters are acquired for all conditions. During the acquisition a stable or a peak-hold averaging method is respectively used for stabilized and transitory conditions.

The blade chord bending spectra are plotted and the frequencies of the peaks are identified.

The helicopter Tail Rotor forcing frequencies are combination of main and tail rotor angular speeds and of natural frequencies of aircraft fuselage modes [Ref. 1] and are related to cyclic inplane or collective out-of-plane modes.

The no recognizable frequencies are suspected to be the inplane cyclic mode frequencies. This procedure is repeated for all the obtained spectra.

Then the spectra are depicted in a 3D plot and in a contour plot format. The anomalies of the trend of the amplitude permit to verify, from a global point of view, the assumed lag cyclic natural frequency behaviour. Finally the relationship found between the cyclic inplane mode frequencies and the cuff pitch angle is plotted.

Frequency and Operational Shape Id. Method -

As described above all the available parameters are used for this analysis. These parameters are re-acquired by the use of a analog/digital converter. This procedure is repeated for all the chosen flight conditions. Different averaging methods are used depending on steadiness or transitoriness of the flight conditions.

The autospectra and crossspectra (computed with reference to one particular stress parameter) calculus is then performed.

Then, employing a running mode analysis, the cyclic motion of each DOF is then investigated. This approach guarantees a fixed phase relationship between the different response signals, using as reference the phase of the reference parameter.

This procedure permits to directly identify the rotor modes from their actual operational deflection shapes, and to track the shifts of the mode frequencies.

Finally lag mode frequencies versus imposed cuff pitch angle relationship is obtained.

5. GTV Results

Most of the expected frequencies had been identified. In Figs 3-4 the chord and beam bending spectra obtained at 21 degrees cuff pitch angle are reproduced in stable and not stable excitation condition. The vertical cursor traces indicate the identified frequencies. The key for the different traces are listed in Fig. 2, where:

- MRev is the Main Rotor rotational speed;
- TRev the Tail Rotor rotational speed;
- n an integer (1, 2, ...);
- b the Main Rotor blades number;
- F_i the i-th natural frequency of the fuselage.

The asterisk indicates the suspected (not recognizable as one of the expected frequencies) cyclic inplane mode frequencies.

Two cyclic lag frequencies had been identified, as due to stack separation of adjacent blade pairs.

In the non stable condition the effects of the forced and free fuselage frequencies are quite clear.

The dimensionless chord bending spectra obtained with impulsive excitation, at different pitch are plotted in Figs 5-10, where the cursor traces mark the probable placement of the two cyclic inplane mode frequencies. The cyclic lag frequencies cross the $2 \times TRev$ at about 13 and 16.5 deg respectively.

In Fig. 11 the dimensionless chord bending stress versus the frequency for different cuff pitch values are plotted in a contour format, where the assumed path of the cyclic lag frequencies is indicated. The same is represented in a 3D plot (Fig. 12).

Unfortunately for the GTV data, the only FIM analysis was performed because of the lack of acquired parameters. So there was not the possibility to verify the real nature of the supposed lag cyclic inplane modes.

6. Prototype Results

The achieved cuff pitch angle range is quite lower than the achieved one during the GTV run.

On the beam and chord bending spectra

(referring to about 19 degrees cuff pitch angle both in stable and in transitory average modes) plotted in Figs 13-14 the vertical cursor traces indicate (with the same legenda described in Fig.2) the identified frequencies. In Fig. 15 the contour plots obtained from both rotations and steady state flight conditions are represented. The FIM assumed lag inplane cyclic mode frequencies paths are indicated by the cursor traces. The cyclic lag frequencies cross the $2 \times TRev$ at about 14 and 16 degrees.

For the prototype data there was the possibility to perform the OSIM analysis. This allowed to recognize the mode shapes.

In the upper part of Figs. 16-19 the first cyclic inplane lag running modes found for different pitch angles are shown. To show the effects due to cyclic lag mode coalescence, in the lower part of the figures the running mode at the same frequency but at different cuff pitch angle (19° or 14°) is shown as well. In the lower part of the Fig. 18 it is evident that the forcing at $2.1 \times TRev$ acts on the cyclic inplane motion. The coalescence with the first inplane Cyclic Tail Rotor mode frequency is denunced by the difference in the shape (in the lower figure part also the mast is moving) and by the jump in the amplitude of the cyclic inplane component of the motion clearly visible (250 vs .75 full scale value) in the upper part.

In Fig. 17 the first inplane cyclic running mode at a value cuff pitch angle of 14 deg is plotted. It occurs at about $2 \times TRev$. At this frequency exists an high forcing acting on collective motion (lower part of the figure). But in the upper part figure is possible to see a modification of the operative mode shape with the addition of a cyclic component in the motion. Generally it was not so easy to recognize the cyclic lag inplane modes in the proximity of $2 \times TRev$.

The two cyclic inplane modes frequencies cross the $2 \times TRev$ at about 14 and 16 deg respectively.

The curves obtained with both the first (FIM) and the second (OSIM) analysis are plotted in Fig.20. It is easy to see that the differencies are quite small. This give confidence in the results of the simplest FIM analysis.

7. Conclusions

The two different methods permit the analysis of the dynamic behaviour of the Tail Rotor lag natural mode frequencies. The first one (FIM) requires the acquisitions of less parameters in respect of the other one (OSIM). However the OSIM allows to reduce the uncertainties of the obtained values.

The two methods have been applied to the analysis of the EH101 GTV and Prototypes Tail Rotor. The behaviour of the GTV and the Prototype are quite similar. In the Fig. 21 the obtained curves are depicted. The pitch-cyclic lag frequency relationships shows that the crossing of the $2 \times T_{Rev}$ happens at a very similar pitch angle values for both the GTV and the Prototype data (particularly for the second cyclic inplane mode). The differences are, probably, due to the different fuselage dynamic behaviours of the prototypes and of the GTV. Furthermore in Fig. 22, where the lag mode frequencies both of the first semirigid and of the final teetering configurations are depicted, is very clear to see that the $2 \times T_{Rev}$ crossing happens at a very more favourable pitch value for the last design solution, as desired.

8. Bibliography

1. R.W. Blake, R.L. Bennet, T.M. Gaffey and R.R. Lynn "Tail Rotor Design. Part II: Structural Dynamic." AHS Journal.
2. D. Banerjee. ITR Methodology Workshop. NASA 20-21 June 1983.
3. R.L. Bialawa. Notes Regarding Fundamental Understandings of Rotorcraft Aerolastic Instability. Proceedings of the 11th ERF, Paper N°62, Sept. 1985.
4. B. Enekl, V. Klöppel. Design Verification and Flight Testing of a Bearingless Soft Inplane Tail Rotor. Proceeding of the 11th ERF, Paper N°40, Sept. 1985.

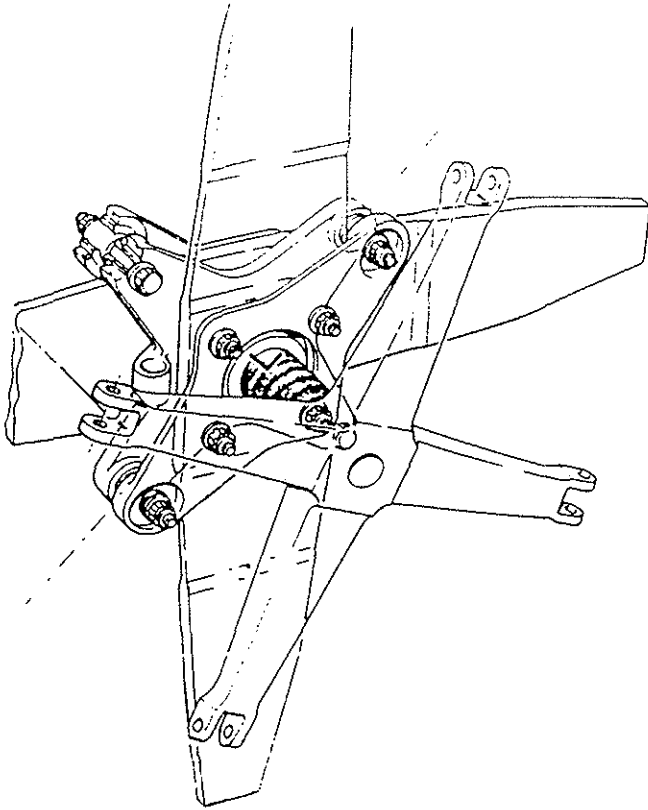


Fig. 1 - EH101 Teetering Tail Rotor.

Blade Mode	Cursor Marker
Coll. out-of-plane	1440Hz
	1480Hz
Cyclic in-plane	11000Hz
	10400Hz
	10800Hz
Coll. out-of-plane	71
Cyclic in-plane	17100Hz

Fig. 2 - Tail Rotor forcing and cursor trace key.

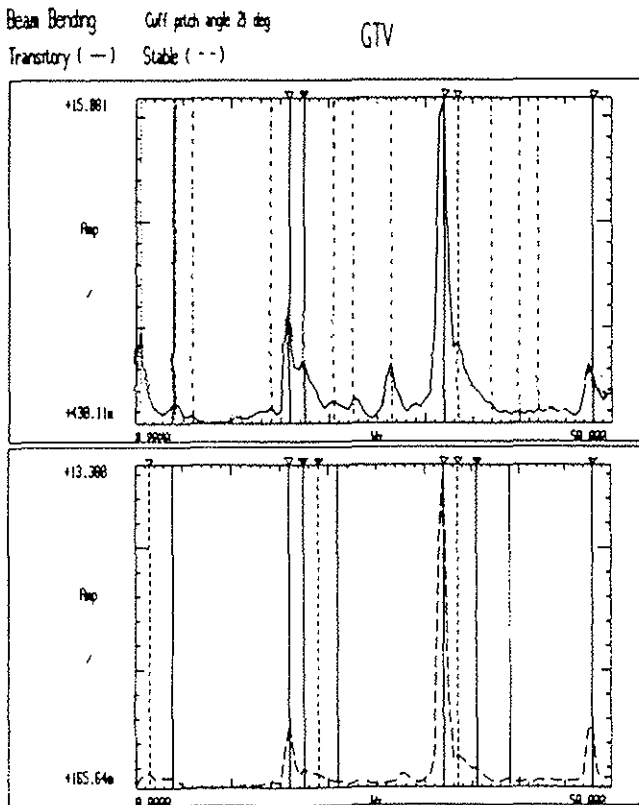


Fig. 3 - GTV Blade Beam Bending Spectra at 21° Pitch Angle both in Transitory and Stable Conditions.

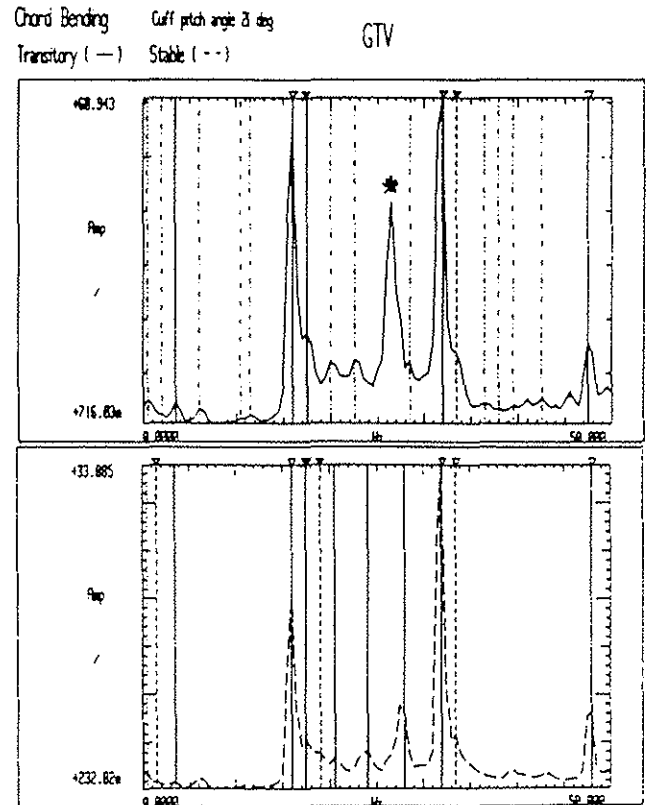


Fig. 4 - GTV Blade Chord Bending Spectra at 21° Pitch Angle both in Transitory and Stable Condition.

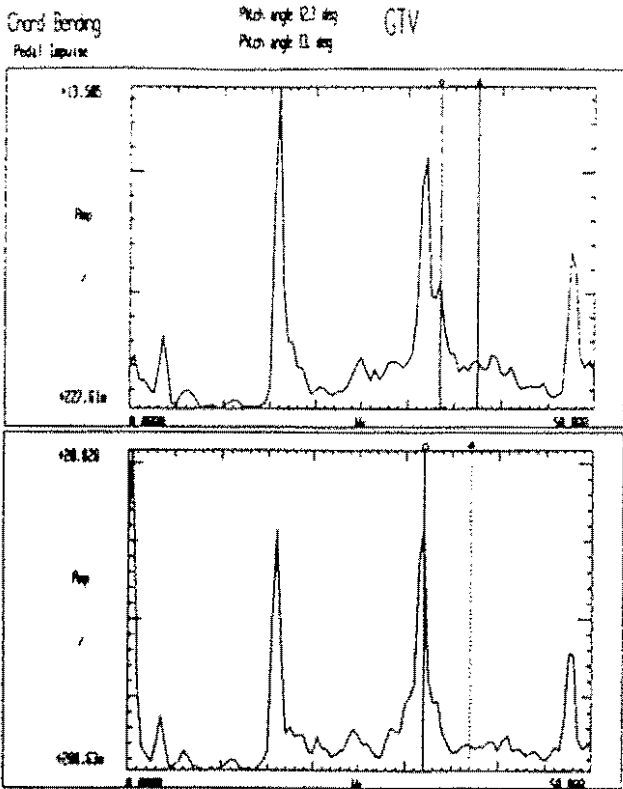


Fig. 5 - GTV Blade Chord Bending Spectra at 12.3' and 13' Pitch Angles. Cyclic Lag Mode Frequencies.

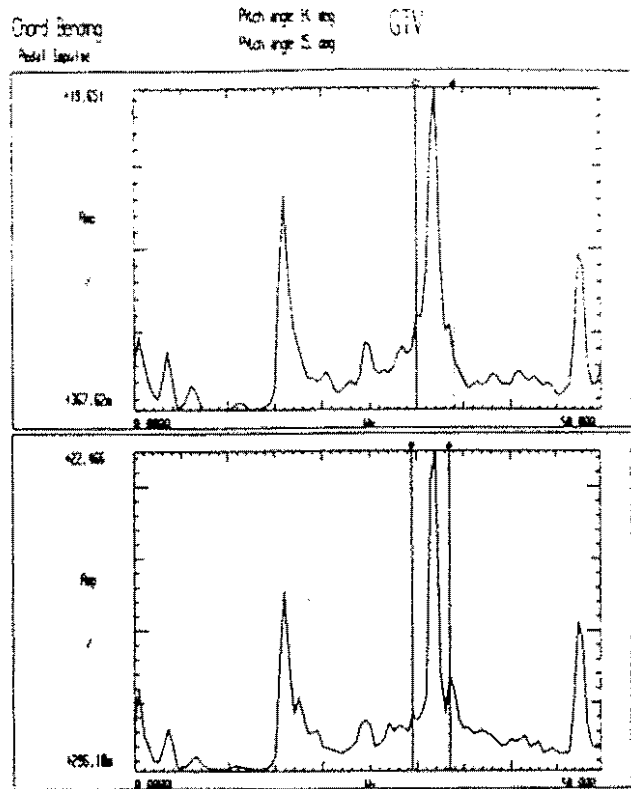


Fig. 6 - GTV Blade Chord Bending Spectra at 14' and 15' Pitch Angles. Cyclic Lag Mode Frequencies.

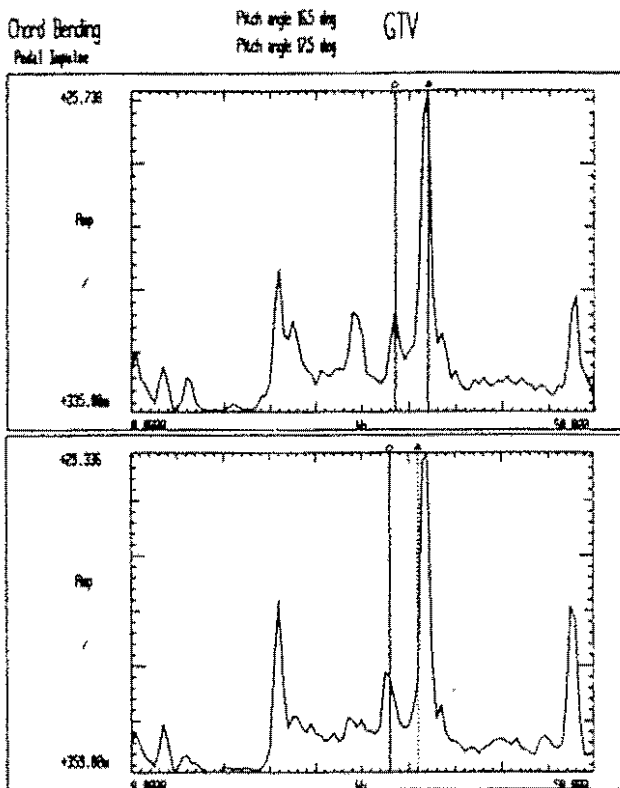


Fig. 7 - GTV Blade Chord Bending Spectra at 16.5' and 17.5' Pitch Angles. Cyclic Lag Mode Frequencies.

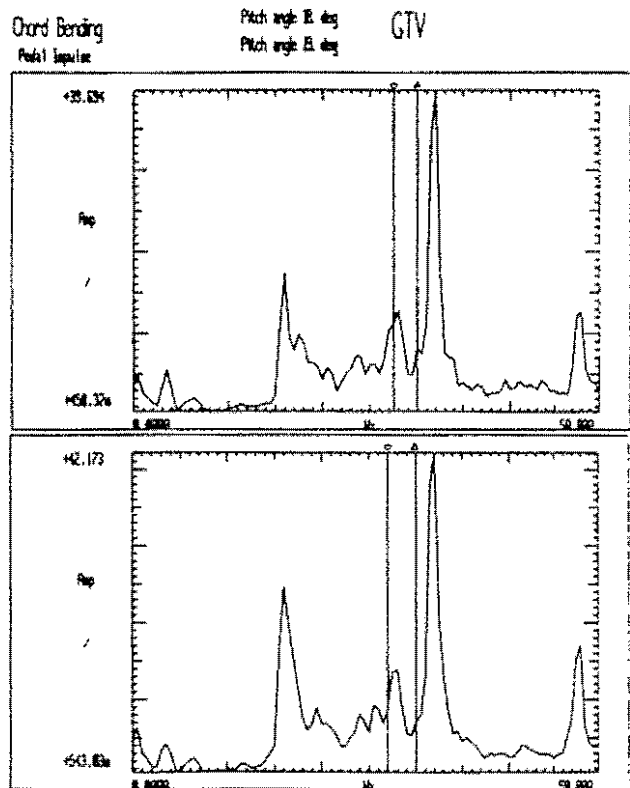


Fig. 8 - GTV Blade Chord Bending Spectra at 18' and 19' Pitch Angles. Cyclic Lag Mode Frequencies.

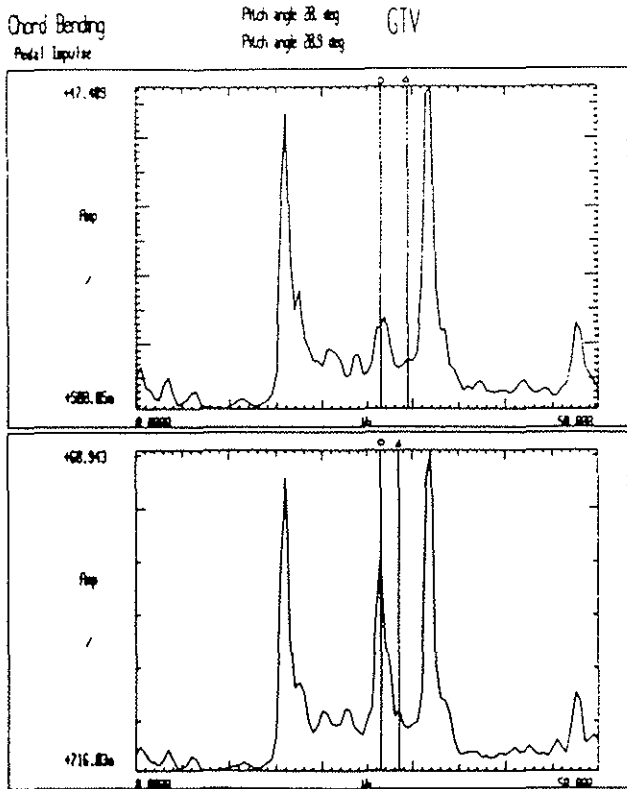


Fig. 9 - GTV Blade Chord Bending Spectra at 20° and 20.9° Pitch Angles. Cyclic Lag Mode Frequencies.

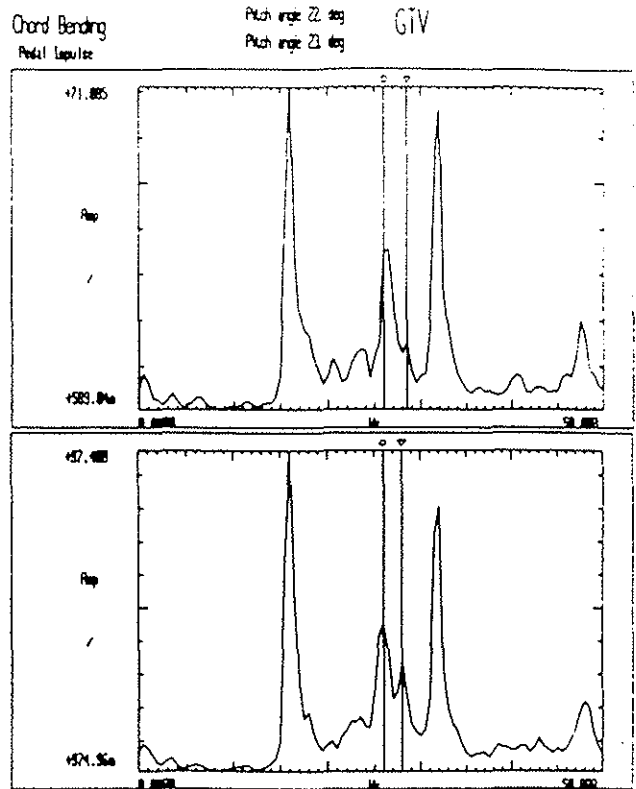


Fig. 10 - GTV Blade Chord Bending Spectra at 22° and 23° Pitch Angles. Cyclic Lag Mode Frequencies.

Chord Bending Spectra Amplitud [log10]

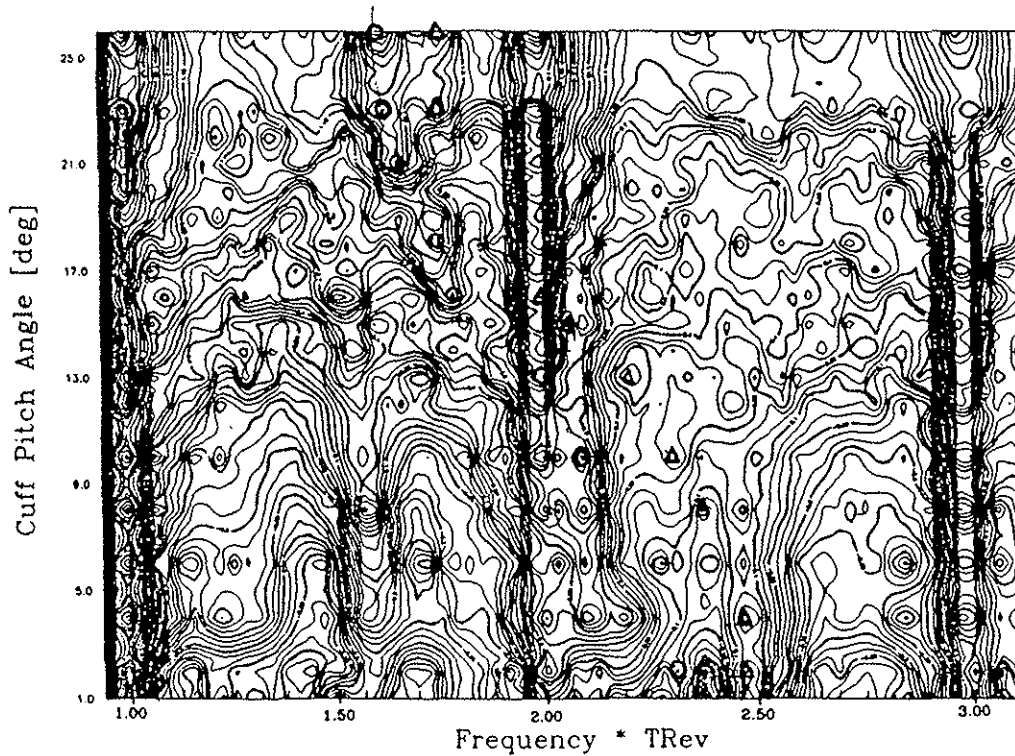


Fig. 11 - GTV Blade Chord Bending Spectra vs Pitch Angle. Location of Cyclic Lag Mode Frequencies.

Chord Bending Spectra

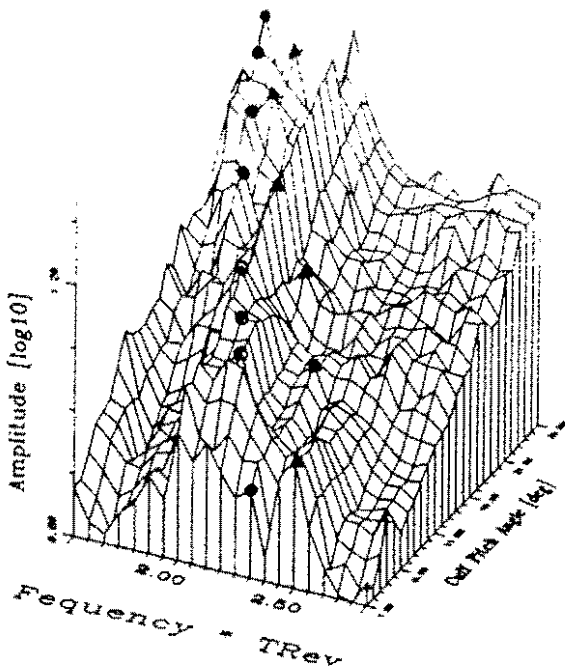


Fig. 12 - GTV Blade Chord Bending Spectra vs Pitch Angle. Location of Cyclic Lag Mode Frequencies.

Beam Bending Transitory () Pitch angle 14.3 deg PP2
Steady () " " " " " "

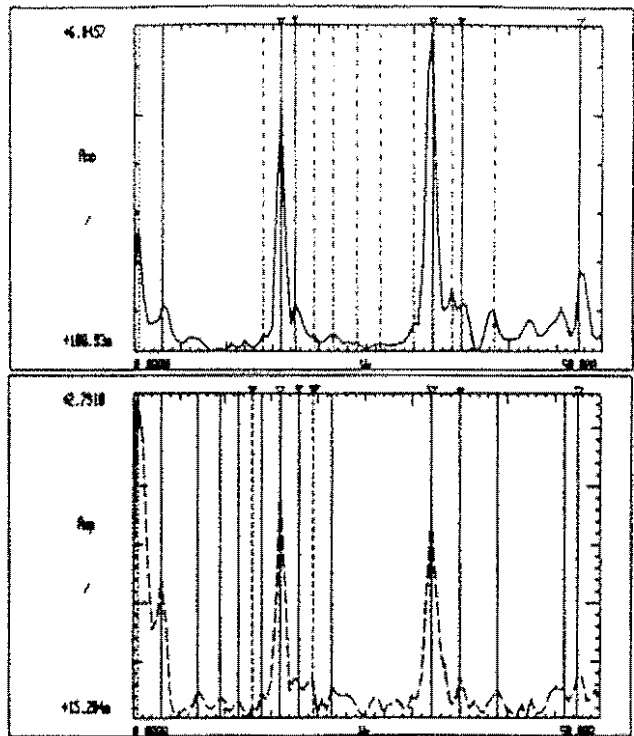


Fig. 13 - Prototype Blade Beam Bending Spectra at about 14° Pitch Angle. Both Steady Flight and Rotation.

Chord Bending Transitory () Pitch angle 14.3 deg PP2
Steady () " " " " " "

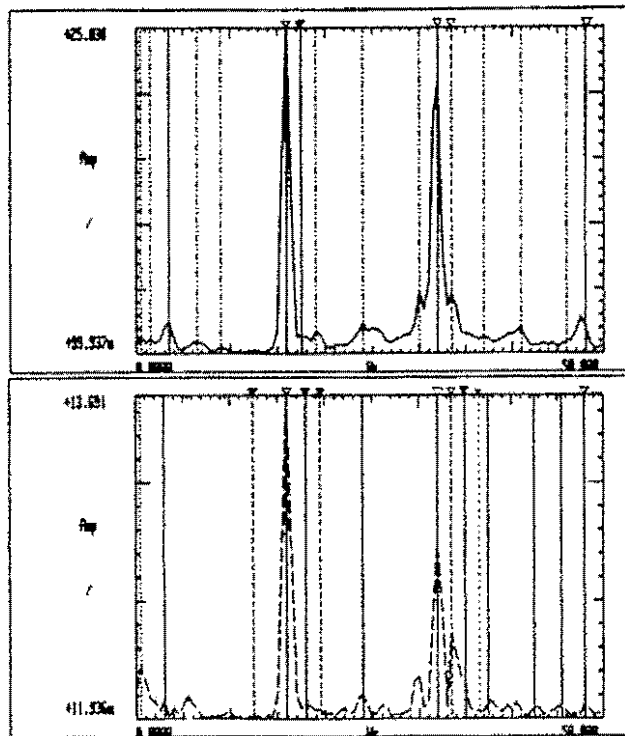


Fig. 14 - Prototype Blade Chord Bending Spectra at about 14° Pitch Angle. Both Steady Flight and Rotation.

Chord Bending Spectra Amplitude [log10]

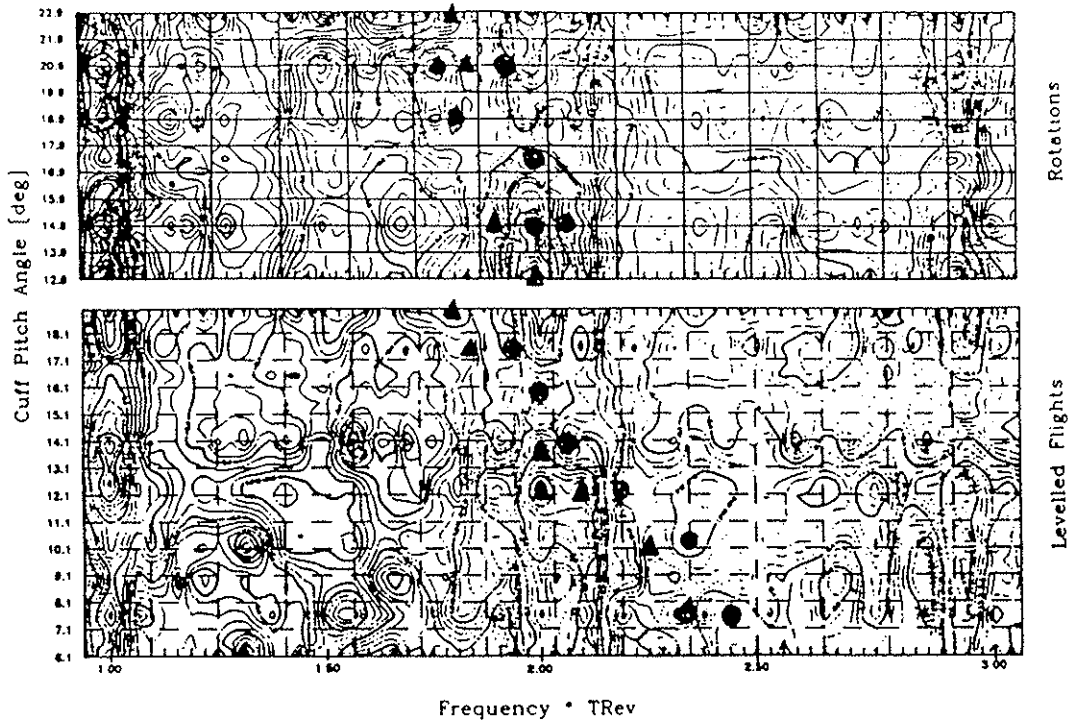


Fig. 15 - Prototype Blade Chord Spectra vs Pitch Angle for both Steady Flight and Rotation. Location of Cyclic Lag Mode Frequencies.

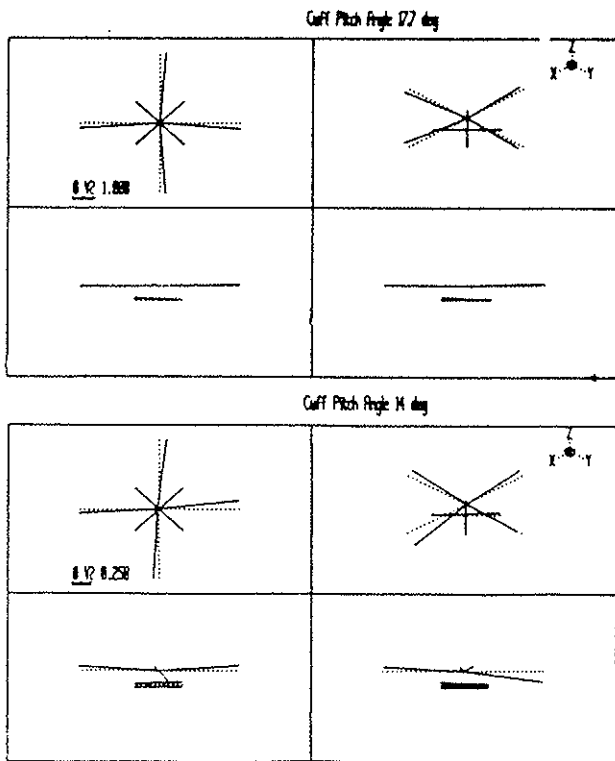


Fig. 16 - Prototype Tail Rotor Operational Shapes at $\approx 1.8 \times TRev$ Hz for 17.7' and 14' Pitch Angles.

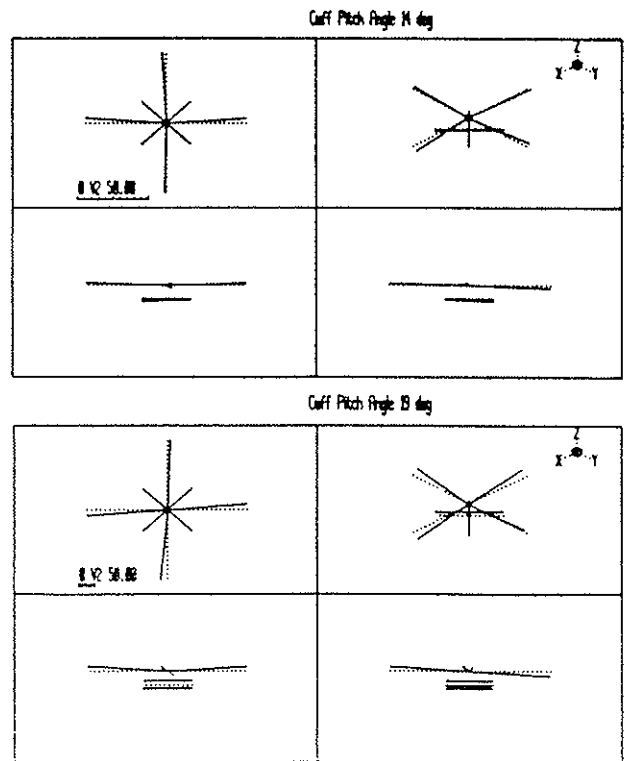


Fig. 17 - Prototype Tail Rotor Operational Shapes at $\approx 2 \times TRev$ Hz for 14' and 19' Pitch Angle.

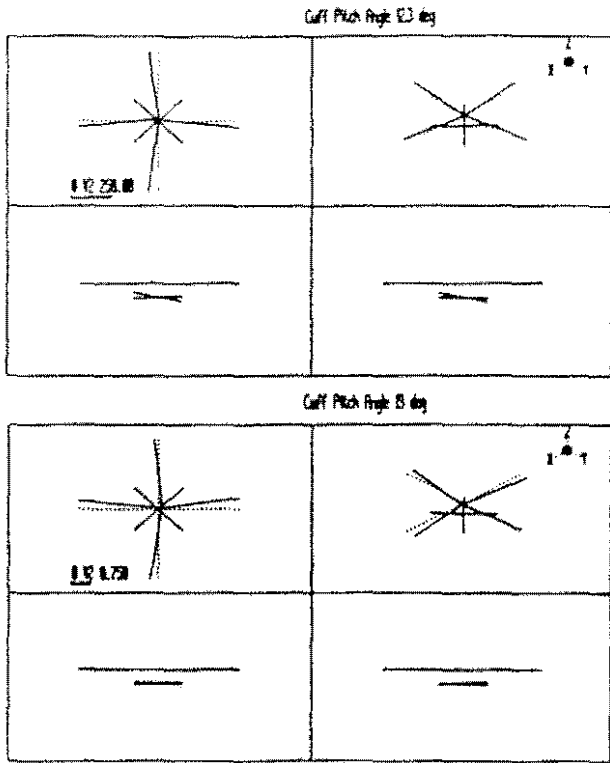


Fig. 18 - Prototype Tail Rotor Operational Shapes at $\approx 2.1 \times TRev$ Hz for 12.3° and 19° Pitch Angles.

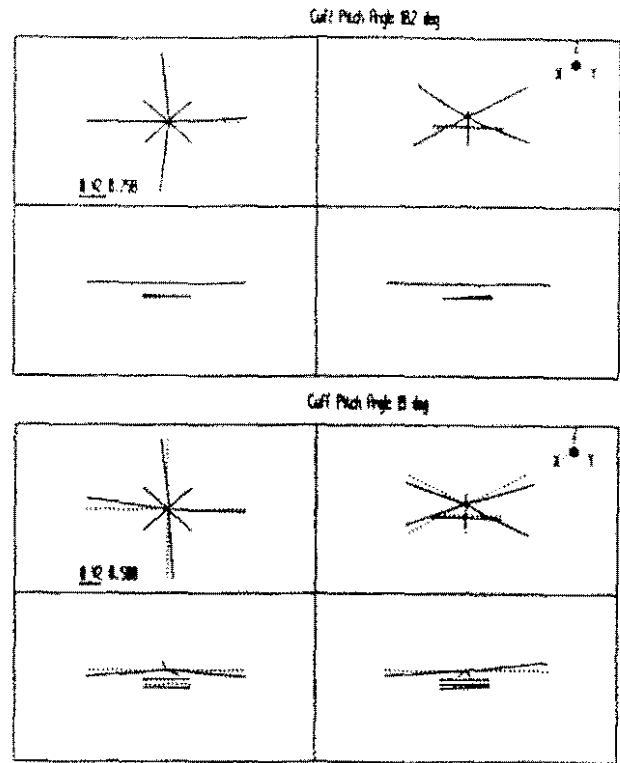


Fig. 19 - Prototype Tail Rotor Operational Shapes at $\approx 2.2 \times TRev$ Hz for 10.2° and 19° Pitch Angles.

EH101 TAIL ROTOR CHORD FREQUENCIES

PP Flight 293 - Cyclic Modes

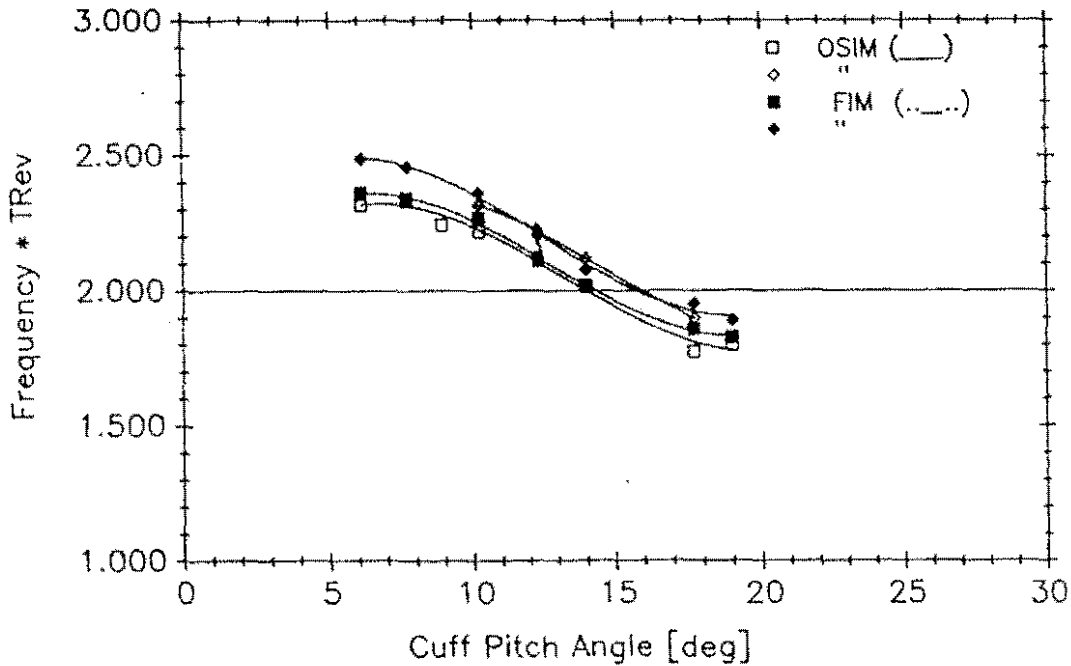


Fig. 20 - Prototype Lag Cyclic Mode Frequencies vs Pitch Angle. (Both FIM and OSIM methods).

EH101 TAIL ROTOR CHORD FREQUENCIES

PP Flight 293 & GTV Run 866 – Cyclic Modes

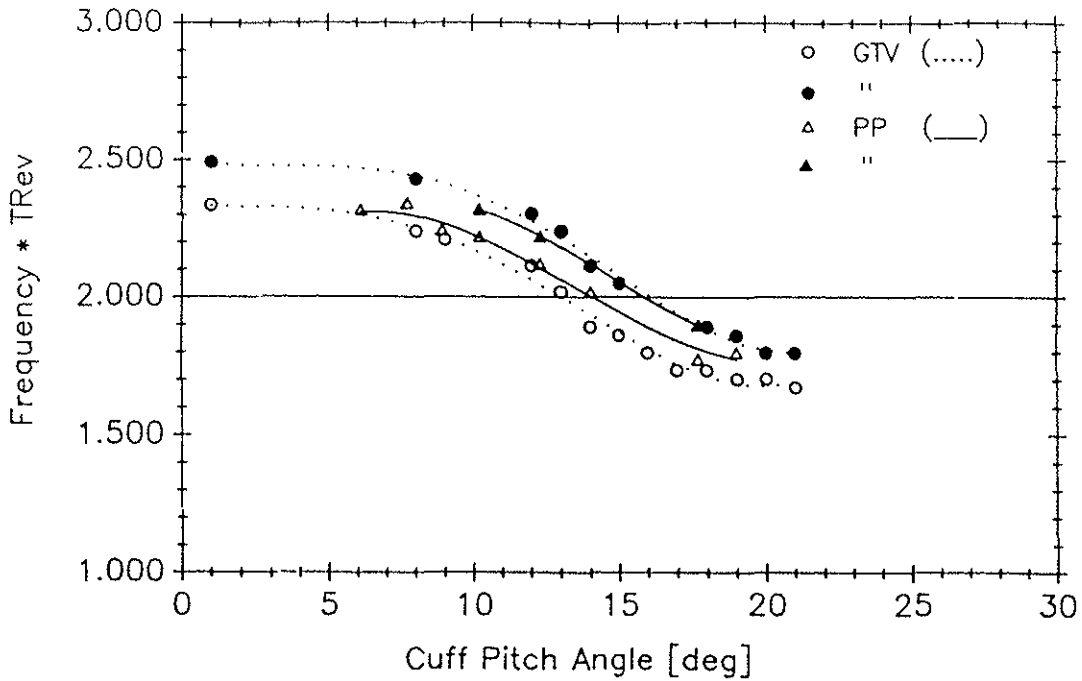


Fig. 21 - Prototype and GTV Cyclic Lag Mode Frequencies vs Pitch Angle.

EH101 TAIL ROTOR CHORD FREQUENCIES

PP semirigid rotor vs GTV(○) and PP(□) teetering ones

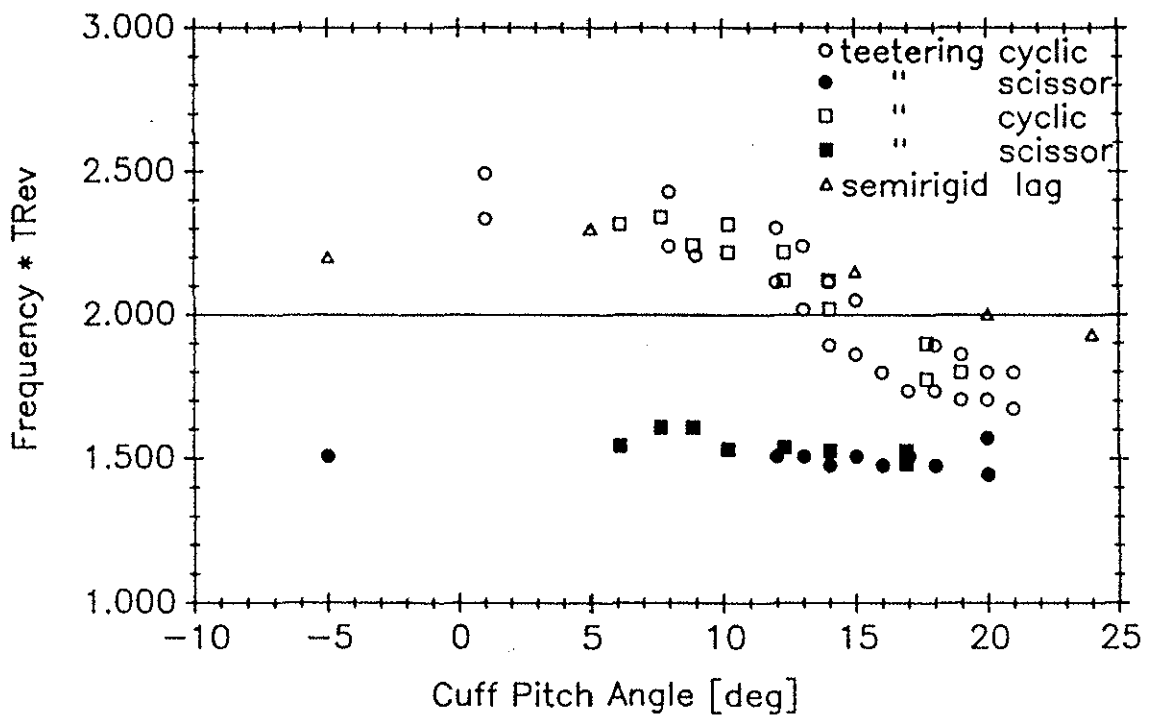


Fig. 22 - Lag Dynamics of both semirigid and teetering rotors.